24th COBEM - 2017

24th ABCM International Congress of Mechanical Engineering
December 3-8, 2017, Curitiba, PR, Brazil

COBEM-2017-2915
APLICATTION OF THE MASKLESS ELECTROCHEMICAL TEXTURING METHOD IN THE REDUCTION OF FRICTION AND WEAR OF THE GRAY CAST IRON

Leonardo Rosa Ribeiro da Silva
Universidade Federal de Uberlândia, Laboratório de Ensino e Pesquisa em Usinagem, Uberlândia, Brasil
leonardo.rrs@gmail.com
Henara Lilian Costa
Universidade Federal do Rio Grande, Escola de Engenharia, Rio Grande, RS, Brasil
henaracosta@furg.br

Abstract. *This work aims to investigate the application of the maskless electrochemical texturing (MECT) in the surface texturization of gray cast iron cylinder liners. Potentiodynamic polarization tests were performed to investigate the possibility os using common table salt insted of pure NaCl as electrolyte, making the process cheaper. In the texturing tests the main parameters of the MECT were optimized for the gray iron, reaching the best results for a distance between the tool and the workpiece of 100 μm, a time of 60 seconds and a voltage of 7.5 V. Finally through Block-on-ring tests was evidenced that surfaces subjected to surface texturing presented lower friction coefficients and wear in relation to surfaces polished mechanically and electrochemically.*

Keywords: *MECT, Lubrication, Friction, Wear, Gray Cast Iron, cylinder liners*

1. INTRODUCTION

Only a small fraction of the energy generated by combustion is effectively utilized in the movement of automotive vehicles (Holmberg, *et al.*, 2012; Holmberg, *et al.*, 2014). The friction between components of an internal combustion engine, especially the tribosystem composed of the cylinder, piston and its rings, is responsible for about 20% of mechanical efficiency losses (Bedajangam and Jadhav, 2013). The topographic control of surfaces in relative motion is an effective way to increase efficiency in tribological systems (Hutchings and Shipway, 1992). Techniques such as honing (Pawlus, *et al.*, 2009) and coating (Ernst and Barbezat, 2008) are already widely used in the reduction of friction and wear of automotive cylinder liners.

Surface texturization can be understood as the production of surface patterns aiming to improve the functional properties of a component (Bruzzone, *et al.*, 2008). Several techniques of surface texturing have been proposed over the years, but it is still necessary to create techniques that are more cost-effective (Costa and Hutchings, 2015). The maskless electrochemical texturing method (MECT) has been shown to be an alternative that combines both low cost and high productivity when compared to laser and photochemical texturing methods (Parreira, *et al.*, 2012).

The objective of this work is to investigate the applicability of the MECT for texturization of gray cast iron automotive cylinders. The tribological gains regarding the friction and wear of textured samples were also evaluated, being compared with mechanically and electrochemically polished samples, through block-on- ring lubricated tests.

2. MATERIALS AND METHODS

2.1 Material of the workpieces

All samples analyzed at this work were obtained from gray cast iron with a perlitic matrix as shown in Fig. 1, with an interlamellar spacing of the perlite of 0.34 μm. The material had a Vickers hardness of 185 ± 2.5 HV, measured at a load of 62.5 kg. The micro hardness of the perlite matrix was 274± 5.1 HV0.1.

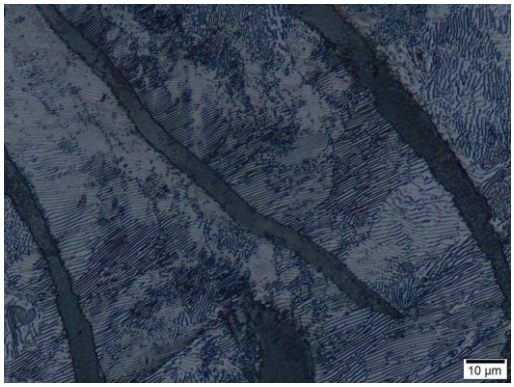

Figure 1. Microstructure of the gray cast iron (Da Silva, 2016).

2.2 Potentiodynamic polarization tests

In order to reduce costs, was investigated the possibility of substitute pure NaCl with common table salt as an electrolyte for MECT, using potentiodynamic polarization tests. All tests were performed at a concentration of 200 $g.L^{-1}$.

The samples were prepared with a cross-section area of 1 cm^2. After that, an electrode was brazed on one side of the sample. The next step was to embed the same in acrylic resin. Finally, the samples were grinded until a final finish obtained with the 2000 grit sandpaper, and then polished with chromium oxide (5 µm). Figure. 2 illustrates the work pieces used in this step. Figure 3 illustrates the plastic beaker used as electrochemical cell to store the electrolyte, as well as the reference electrode (saturated calomel), the counter electrode (platinum net) and the work piece.

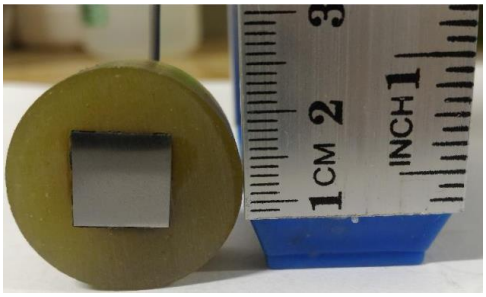

Figure 2. Sample used in the potentiodynamic polarization tests (Da Silva, 2016).

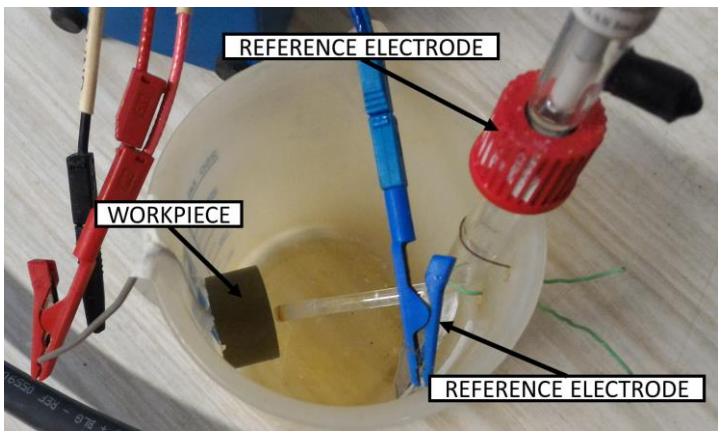

Figure 3. Electrochemical cell used during the Potentiodynamic Polarization Tests (Da Silva, 2016).

2.3 Adaptation of the MECT technique for automotive cylinders liners made of gray cast iron

The specimens were made based on the Honda CRF 450® motorcycle cylinders liners. The cylinders were 97.5 mm high and had an internal diameter of approximately 96.5 mm. The replicates had their internal surfaces grinded with the aid of a lathe up to 2000 grit sandpaper, and then polished with chromium oxide (5 µm). The samples were divided into three groups with 96.1, 96.2 and 96.3 mm internal diameter, being one sample shown in the Fig. 4.

Figure 4. Replica of the cylinder liner (Da Silva, 2016).

The necessary apparatus for application of the MECT technique in the automotive cylinders is shown in Fig. 5. A DC power source (1) generates the voltage necessary for the electrochemical dissolution, with the negative pole being connected to the tool (2) and the positive to the sample (3). A pump (5) pumps the electrolyte (6) through small gaps in the tool and electrifies, thus texturizing the sample. An electronic circuit (4) is used to pulse the signal, maximizing the efficiency of the anodic dissolution.

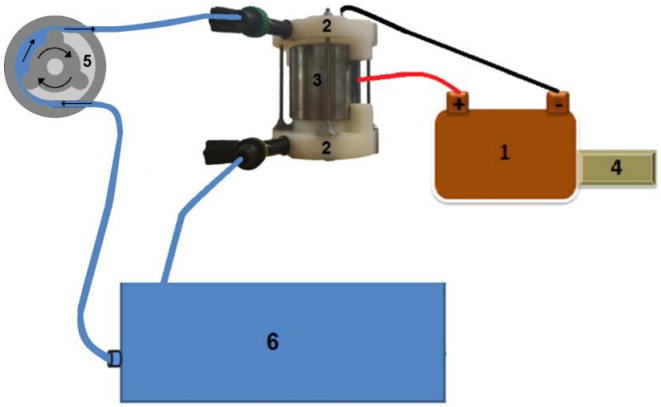

Figure 5. Experimental apparatus for application of the MECT technique in the automotive cylinders: (1) DC power supply, (2) texturing chamber, (3) Replica of the cylinder liner, (4) pulse generator, (5) peristaltic pump, (6) electrolyte (Da Silva and Costa, 2017a).

The texturing chamber is shown in more detail in Fig. 6, being (1) and (2) the top and the bottom covers made of Nylon, (3) the work piece, (4) the tool, which was made of austenitic stainless steel class 304 with 96 mm of diameter. The inlet and outlet of the electrolyte was carried out by ducts (5) and (6), respectively. The tool was laser drilled with V-shaped patterns, since this texturization pattern proved to be very effective according to Costa e Hutchings (2007). During the testes where evaluated as parameters the best gap between the tool and the workpiece, the voltage and the texturing time, as shown in Fig. 7.

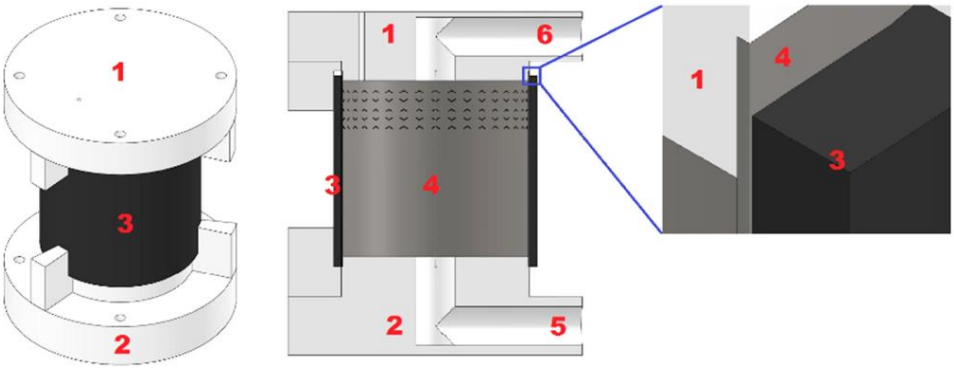

Figure 6. Experimental apparatus for application of the MECT technique in the automotive cylinders: (1) Top cover, (2) bottom cover, (3) work piece, (4) tool, (5) inlet and (6) outlet of electrolyte (Da Silva, 2016).

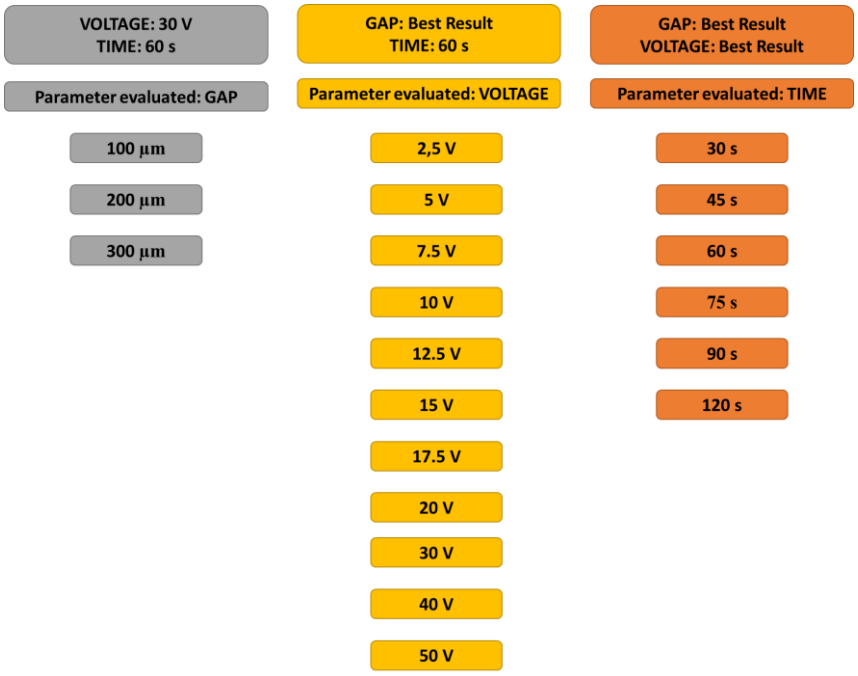

Figure 7. Parameters evaluated during the surface texturing tests (Da Silva, 2016).

2.4 Tribological tests

The tribological tests were performed using a FALEX block-on-ring tribometer according to Fig. 8, at a normal load of 343 N and a total time of 20 minutes per test. The tests were performed using a SAE 40 mineral-based lubricant without additives, having a viscosity (η_o) ranging from 159.9 cSt at 40 ° C to 15.2 cSt at 100 ° C. The ring speeds evaluated were 200 and 600 rpm, since for the contact geometry of the test, they give the lower and upper limits of the mixed lubrication regime. The specimens were fabricated in accordance with ASTM D2714 - 94 (2014), having their surfaces polished to a surface finish of S_q = 0,098 ± 0,004 µm.

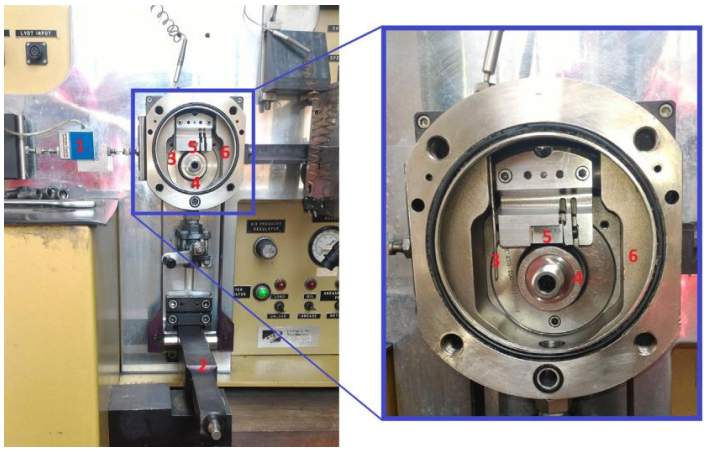

Figure 8. FALEX® block-on-ring tribometer tests (Da Silva, 2016).

3. RESULTS

3.1 Potentiodynamic polarization tests

The cathodic-anodic behavior of the gray cast iron is shown in Fig. 9. It can be seen that the potentiodynamic curves for common table salt and for pure NaCl showed similar behavior, and the corrosion potential for all the tests was about - 0.74 V. the passivation observed at the end of the test is due to carbon accumulation derived detachment of the graphite flakes on the work surface, a phenomenon also observed during previous texturing tests where relatively high voltages and currents have been used in plane gray cast iron samples, as shown in Fig. 10.

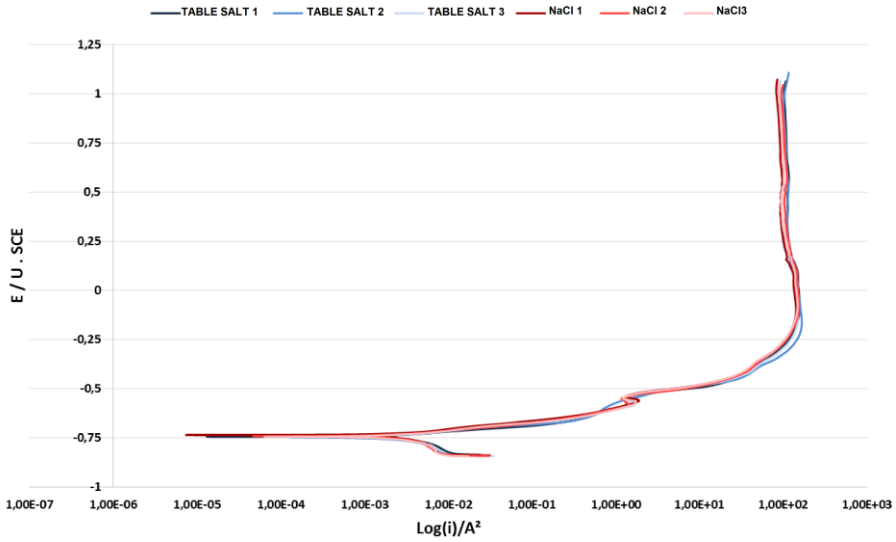

Figure 9. Potentiodynamic polarization tests (Da Silva, 2016).

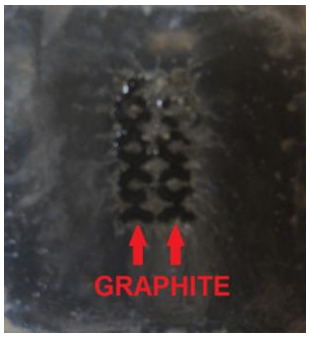

Figure 10. Graphite accumulation (Da Silva and Costa, 2017a).

3.2 Adaptation of the MECT for automotive cylinders liners

The effect of the GAP is illustrated in Fig. 11. By visual analysis it was observed that the lower GAP showed a better resolution of the V-patterns. Another indication that the lower GAP obtained the best performance was that this parameter had the lowest surface roughness in the regions external to the surface patterns inserted, as shown in Fig. 12. Both facts are explained by the lower GAP allow lower dispersion of the electrolyte jet.

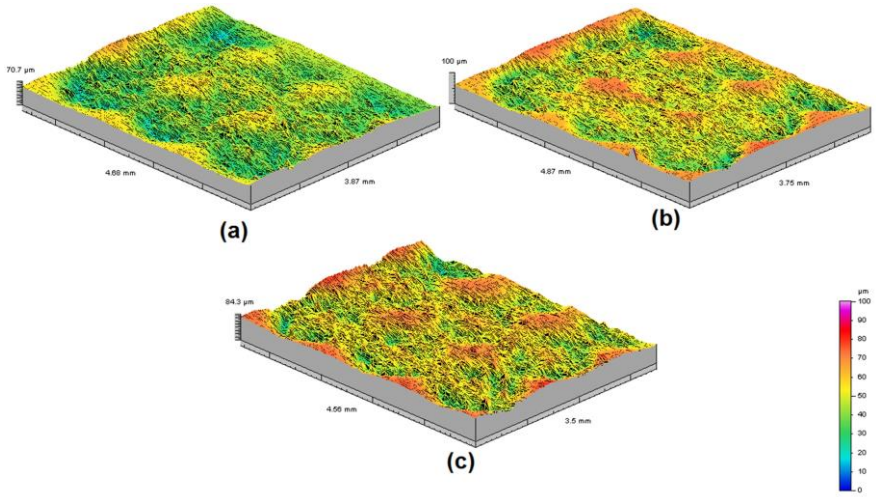

Figure 11. 3D topography for different gaps: (a) 100 µm; (b) 200 µm; (c) 300 µm.(Da Silva and Costa, 2017a).

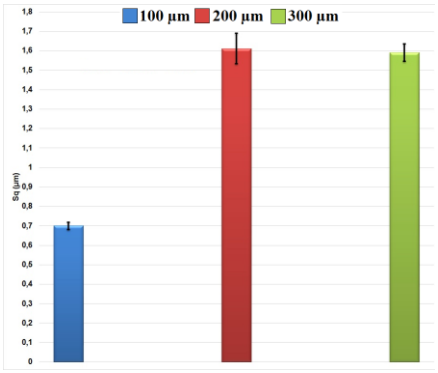

Figure 12. 3D rms roughness (S_q) outside the pockets. (Da Silva and Costa, 2017a).

The effect of the voltage is illustrated in Fig. 13. It is observed that voltages above 20 V did not present well-defined V patterns, since the high anodic dissolution rates led to the creation of passive regions (similar to Fig. 10) , which lead to the electrolyte to dissolve not the desired location, but the adjacencies. In order to parameterize the results, the relationship between the depth and the width of the inserted patterns (R_{dw}) was taken as quality criterion, being desired patterns with the highest values of this parameter and also lower surface roughness in the regions outside the v-patterns. According to Fig. 14, the voltage of 7.5 V presented the best results, since even though it did not present the highest value of R_{dw}, it presented the best relation of this parameter and surface roughness outside the v-patterns.

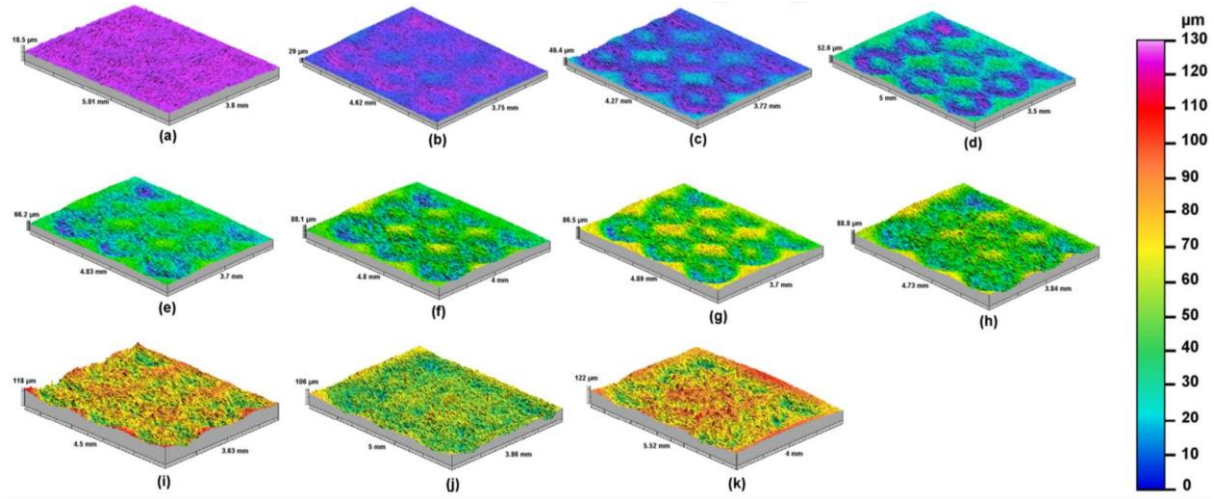

Figure 13. Topographic maps of textured surfaces: (a) 2.5 V; (b) 5 V; (c) 7.5 V; (d) 10 V; (e) 12.5 V; (f) 15 V; (g) 17.5 V; (h) 20 V; (i) 30 V; (j) 40 V; (k) 50 V (Da Silva and Costa, 2017a).

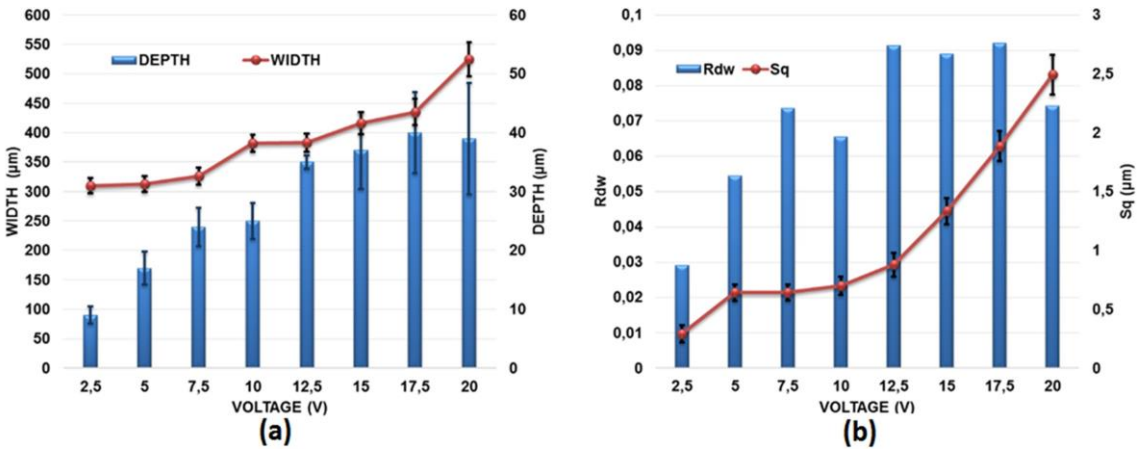

Figure 14. Texture geometry parameters as a function of voltage: (a) depth and width; (b) ratio between depth and width (R_{dw}) and S_q (Da Silva and Costa, 2017a).

Finally, the effect of the texturing time is illustrated in Fig. 15. As a qualitative parameter of the surface patterns produced, the parameter R_{dw} and the roughness of the adjunctive regions were again used, as shown in Fig 16. It is observed that the longer dissolution times lead to a slight increase in depth and a much more pronounced increase in both the width of the patterns as well as the roughness in the adjunctive regions. This can again be explained by the fact that longer dissolution times lead to the occurrence of passive regions, which prevent an accurate anodic dissolution in the desired places. Based on these parameters, the time of 60 seconds was chosen as the most effective for the process.

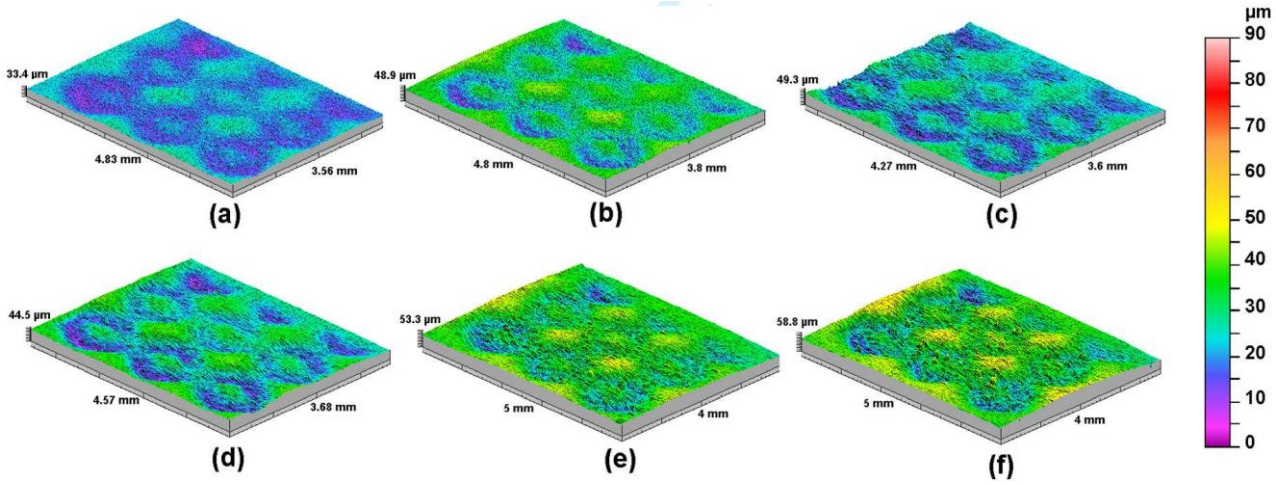

Figure 15. Topographic maps of textured surfaces: (a) 30 s; (b) 45 s; (c) 60 s; (d) 75 s; (e) 90 s; (f) 120 s (Da Silva and Costa, 2017a).

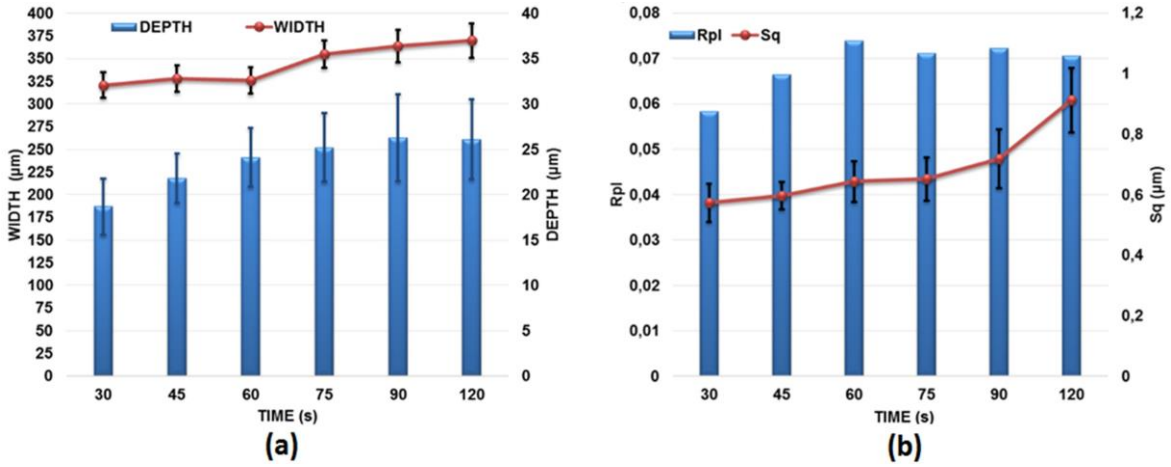

Figure 16. Texture geometry parameters as a function of time: (a) depth and width; (b) ratio between depth and width (R_{dw}) and S_q (Da Silva and Costa, 2017a).

3.3 Tribological tests

Figure 17 illustrates the coefficient of friction over the time for the block-on-ring tribological tests. The initial peaks of friction during the run-in period were smaller for the electrochemically polished and surface textured samples, as these processes expose graphite flakes from the matrix, thus enhancing the effect of this material as a solid lubricant. After this initial period, a drastic drop in the coefficient of friction was observed, with the textured samples having the smallest values and the mechanically polished the largest. This is due to the fact that surface textures act as hydrodynamic micro-bearings, thus increasing the thickness of the lubricating film. This is especially observed at 600 rpm, because the higher speed generates higher hydrodynamic pressure, enhancing this effect. After a certain test time all the samples started to present similar coefficient of friction, since the wear of the block leads to the conformity of the contact between the block and the ring, causing the hydrodynamic effect from this conformity to override both the effect of the surface textures and the exposed graphite flakes.

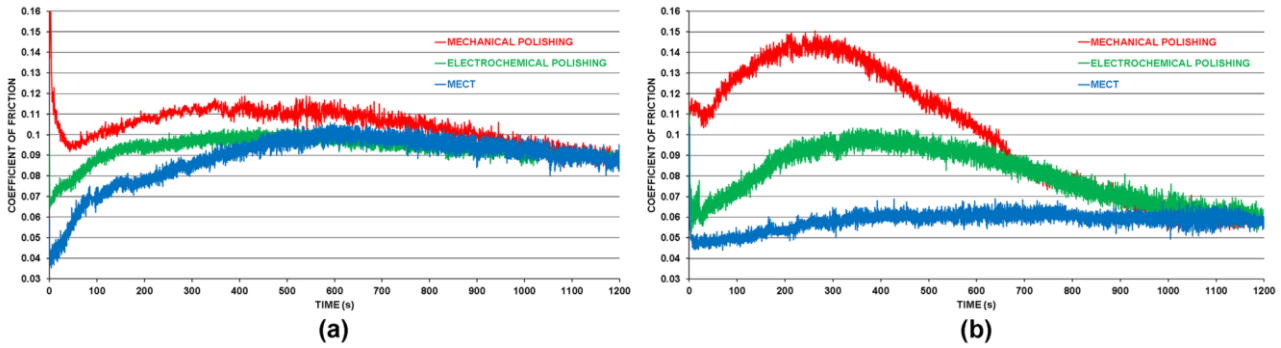

Figure 17. Friction coefficient versus time: (a) 200 rpm; (b) 600 rpm (Da Silva and Costa, 2017b).

Figures 18 and 19 illustrate the wear marks from the tests for the 200 and 600 rpm respectively. It was observed that for both sliding velocities investigated, the textured samples had the smallest worn volume and the mechanically polished the largest. In both conditions there still remains of the v-patterns in the wear marks for the surface textured samples.

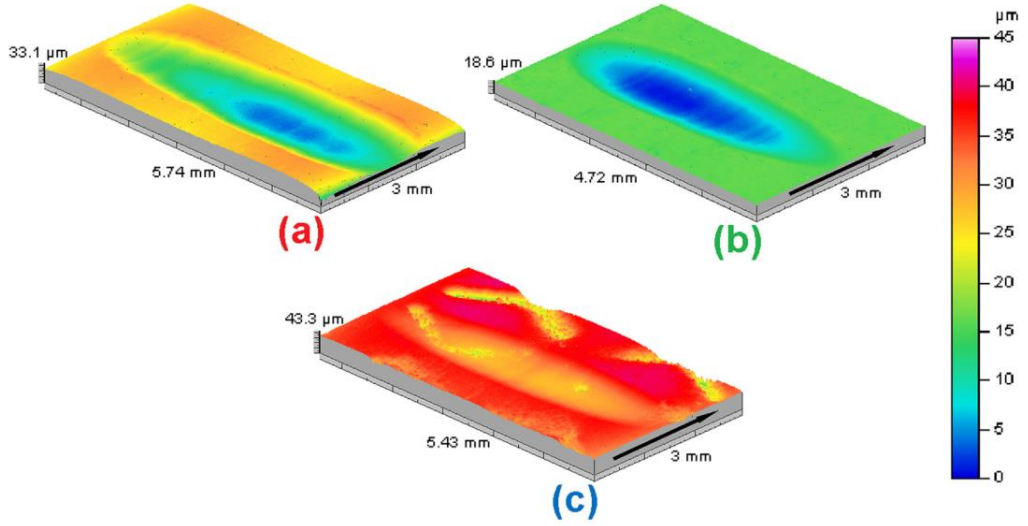

Figure 18. Topography of the wear scars on the blocks after the tests at 200 rpm: (a) mechanical polishing; (b) electrochemical polishing; (c) MECT. (Da Silva and Costa, 2017b).

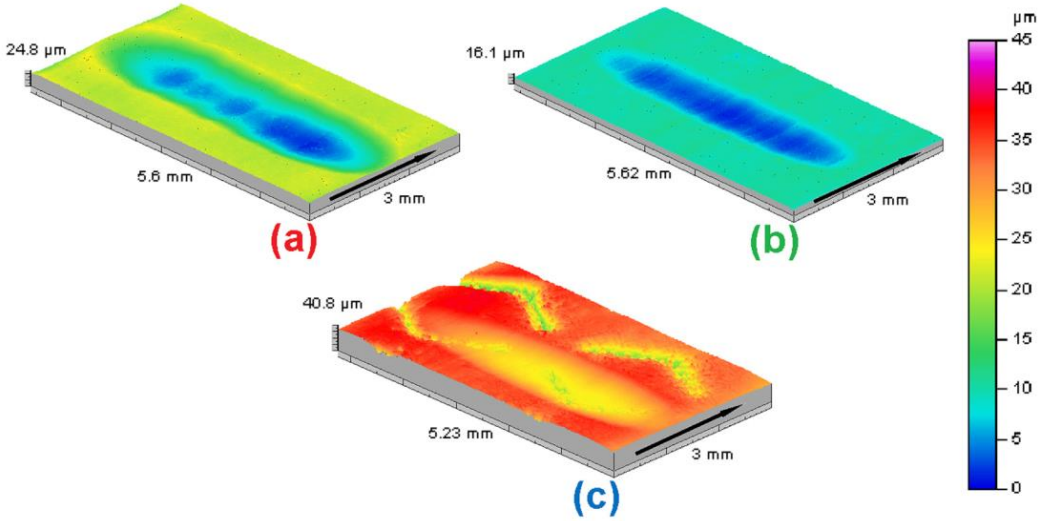

Figure 19. Topography of the wear scars on the blocks after the tests at 600 rpm: (a) mechanical polishing; (b) electrochemical polishing; (c) MECT. (Da Silva and Costa, 2017b).

The wear rates are shown in Fig. 20, and it is observed that, as expected, higher rotation speeds lead to higher hydrodynamic pressures and lower wear, having the textured samples presented the best tribological performance and the mechanically polished samples the worst. The higher hydrodynamic pressures of the tests at 600 rpm, however, led to a higher texturization effectiveness, both through the synergy of this pressure increase with the hydrodynamic micro-bearing effect of the textures, as well as the lower wear rates provide longer service life to these surface patterns before they worn out to the point of losing their effectiveness.

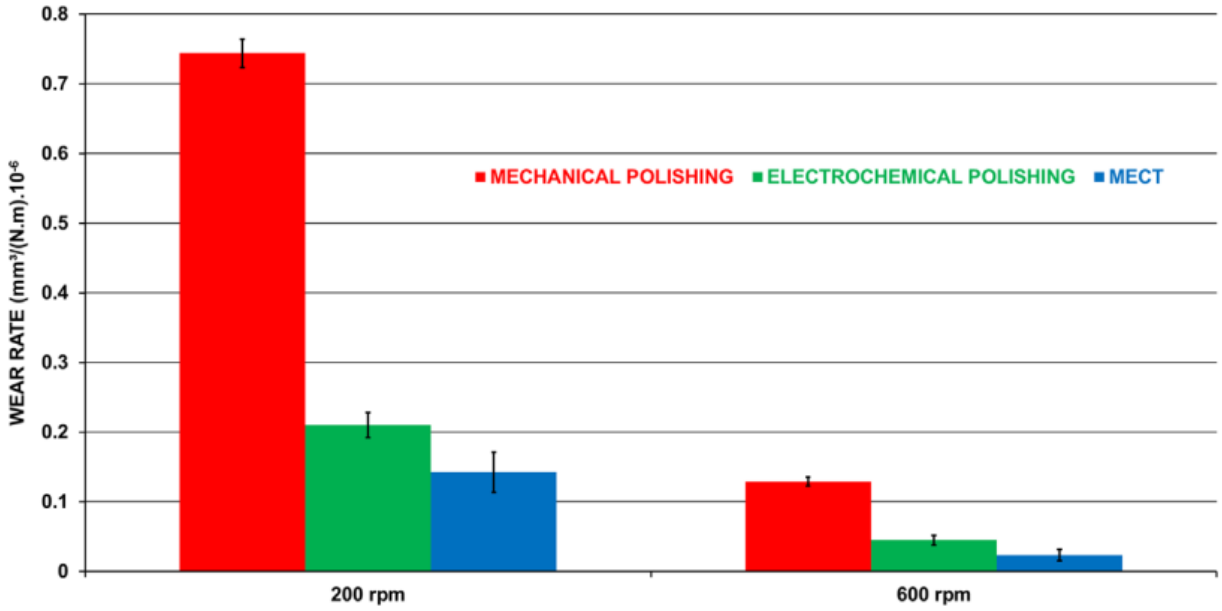

Figure 20. Volume wear rates (Da Silva and Costa, 2017b).

4. CONCLUSIONS

- Common table salt can be effectively used as substituent to pure NaCl in the process of surface texturization of gray cast iron by the MECT method.
- The best surface texturization parameters for gray cast iron were a GAP of 100 μm, a voltage of 7.5 V and a time of 60 seconds.
- Surface texturization was more effective in the reduction of friction and wear when compared to mechanical and electrochemical polishing processes.

5. ACKNOWLEDGEMENTS

The authors would like to thank CAPES, CNPQ and FAPEMIG financial support to carry out this project.

6. REFERENCES

ASTM. Standard Test Method for Calibration and Operation of the Falex Block-on-Ring Friction and Wear Testing Machine. ASTM International. West Conshohocken. D2714-94 2014.

Bedajangam, S.; Jadhav, N. Friction losses between piston ring-liner assembly of internal combustion engine: a review. International Journal of Scientific and Research Publications, v. 3, n. 6, p. 1-3, 2013.

Bruzzone, A. et al. Advances in engineered surfaces for functional performance. CIRP Annals-Manufacturing Technology, v. 57, n. 2, p. 750-769, 2008. ISSN 0007-8506.

Costa, H.; Hutchings, I. Hydrodynamic lubrication of textured steel surfaces under reciprocating sliding conditions. Tribology International, v. 40, n. 8, p. 1227-1238, 2007. ISSN 0301-679X.

Costa, H.; Hutchings, I. Some innovative surface texturing techniques for tribological purposes. Proceedings of the Institution of Mechanical Engineers, Part J: Journal of Engineering Tribology, v. 229, n. 4, p. 429-448, 2015. ISSN 1350-6501.

Da Silva, L.; Costa, H. Maskless Electrochemical Texturing of Automotive Cylinders. Materials Performance and Characterization, v. 6, n. 2, 2017a. ISSN 2165-3992.

Da Silva, L.; Costa, H. Tribological behavior of gray cast iron textured by maskless electrochemical texturing. Wear, v. 376, p. 1601-1610, 2017b. ISSN 0043-1648.

Da Silva, L. R. R. Texturização superficial de cilindros automotivos. 2016.

Ernst, P.; Barbezat, G. Thermal spray applications in powertrain contribute to the saving of energy and material resources. Surface and Coatings Technology, v. 202, n. 18, p. 4428-4431, 2008. ISSN 0257-8972.

Holmberg, K.; Andersson, P.; Erdemir, A. Global energy consumption due to friction in passenger cars. Tribology International, v. 47, p. 221-234, 3// 2012. ISSN 0301-679X. Disponível em: < http://www.sciencedirect.com/science/article/pii/S0301679X11003501 >.

Holmberg, K. et al. Global energy consumption due to friction in trucks and buses. Tribology International, v. 78, p. 94-114, 10// 2014. ISSN 0301-679X. Disponível em: < http://www.sciencedirect.com/science/article/pii/S0301679X14001820 >.

Hutchings, I. M.; Shipway, P. Tribology: friction and wear of engineering materials. 1992.

Parreira, J.; Gallo, C.; Costa, H. New advances on maskless electrochemical texturing (MECT) for tribological purposes. Surface and Coatings Technology, v. 212, p. 1-13, 2012. ISSN 0257-8972.

Pawlus, P.; Cieslak, T.; Mathia, T. The study of cylinder liner plateau honing process. Journal of Materials Processing Technology, v. 209, n. 20, p. 6078-6086, 2009. ISSN 0924-0136.

7. RESPONSIBILITY NOTICE

The authors are the only responsible for the printed material included in this paper.